Force Controllable Hydro-Elastic Actuator

David W. Robinson and Gill A. Pratt

MIT Leg Laboratory
545 Technology Sq. Rm 006, Cambridge, MA 02139 USA
http://www.ai.mit.edu/projects/leglab/

Abstract— **We present a hydro-elastic actuator that has a linear spring intentionally placed in series between the hydraulic piston and actuator output. The spring strain is measured to get an accurate estimate of force. This measurement alone is used in PI feedback to control the force in the actuator. The spring allows for high force fidelity, good force control, minimum impedance, and large dynamic range.**

A third order linear actuator model is broken into two fundamental cases: fixed load – high force (forward transfer function), and free load – zero force (impedance). These two equations completely describe the linear characteristics of the actuator. This model is presented with dimensional analysis to allow for generalization. A prototype actuator that demonstrates force control and low impedance is also presented. Dynamic analysis of the prototype actuator correlates well with the linear mathematical model.

This work done with hydraulics is an extension from previous work done with electro-mechanical actuators.

Keywords— **Series Elastic Actuator, Force Control, Hydraulic Force Control, Biomimetic Robots**

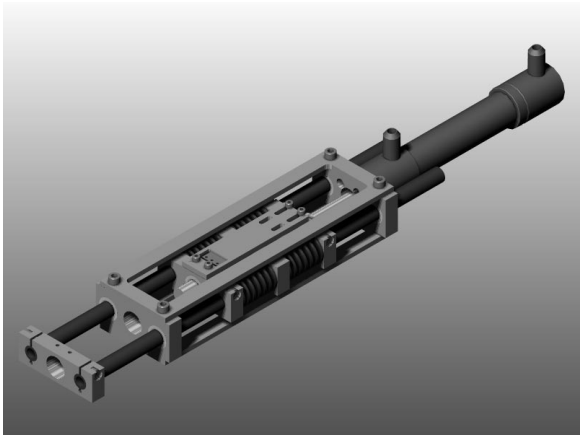

Fig. 1. Prototype Actuator CAD model. A 20MPa pressure source is connected to a MOOG series 30 flow control servo valve which has a bandwidth of about 200 Hz. The piston is coupled to the output through four die compression springs. The spring compression is measured with a linear potentiometer which implies force.

I. Introduction

ROBOT force control and force controllable actuators typically reside in the electro-mechanical domain for several reasons. EM motors are well understood and can typically be modeled as linear systems which makes control significantly easier. They have very fast response times and are operationally clean. Unfortunately, EM motors have very low torque density and can only achieve high power density when run at high speed. Most robot force control tasks, however, run at low speeds and high forces which leads to the use of transmissions or gear reductions. Transmissions introduce many undesirable effects such as friction, reflected inertia and backlash, all of which create torque noise. In addition, transmissions decrease backdrivability or increased impedance, which is a measure of the actuator's force sensitivity. In summary, transmissions are problematic when trying to achieve good force control.

While EM motors with a transmission can achieve a measure of high force and power density, it is well known that hydraulic systems provide a power and force density that is far superior any other present-day actuator technology [1]. Furthermore, hydraulics can generate high loads with moderate response times and can hold those loads indefinitely with very little use of power. This is something that would causes extreme heat generation in an EM motor. The downside to hydraulics is its non-linearity, inherent complexity, and messiness (especially in the case of a system failure.) Hydraulics, similar to EM motors and transmissions, also have high impedance and are difficult if not impossible to backdrive. Therefore, hydraulics have typically not been used in robotic force control.

Previous actuator research in the Leg Laboratory focused in the electro-mechanical domain. From this work came the development of *Series Elastic Actuators* [2], [3]. These force controllable actuators have an intentional spring in between the motor transmission and the actuator output. By controlling the deflection of the spring, a simple control algorithm can generate excellent force control. The spring reduces large force bandwidth. However, many biomimetic robots only need high forces within a limited bandwidth. In exchange for this reduction in bandwidth, Series Elastic Actuators are low motion, high force density, high power density actuators with good force control, im-

pact tolerance and low impedance.

Following the success of EM series elastic actuators, a similar idea of putting a spring in series with a piston is applied to hydraulics. This paper documents the creation of a *Hydro-elastic Actuator* which is a force controllable hydraulic actuator. With a very simple proportional-integral controller using the deflection of the spring for feedback, the actuator has very low impedance thus making the controlled system backdrivable and very force sensitive. It can also produce any specified force up to 2500N maintaining the same backdrivability at the higher forces. This prototype actuator is pictured in figure 1. The prototype actuator is compared to a mathematical model and simulation which is formulated in non-dimensional terms for generality.

II. Related Force Controllable Actuators

A. Electro-Mechanical Actuators

Many people have used compliant actuators or have studied the control of robots with flexible links or compliant joints [4], [5], [6], [7], [8]. This work has been mostly concerned with mitigating the effect of the compliance rather than taking advantage of it.

The highest performance force controlled actuator has been a brushless DC motor rigidly connected to a robot link, also know as direct-drive [9]. These actuators eliminate friction and backlash, typical of motors with transmissions. To compensate for the loss of transmission, direct-drive actuators must be large in order to achieve adequate torque. This means increased motor mass and cost.

Howard [10] introduced the idea of measuring springs in series with an actuator's output by monitoring the displacement between actuator output and motor position, thus inferring spring deflection. This differential measurement is error prone because there is noise between those two points due to the transmission.

Pratt and Williamson [2], [11] developed Series Elastic Actuators by directly measuring the strain of a spring in series with transmission and actuator output. They pointed out that the actuators can trade off small motion bandwidth for good force control. Also, since the spring deforms a significant amount, the fidelity compared to typical strain gauge structures for force control is much higher.

B. Hydraulic Actuators

Springs and other compliant mechanisms have also been used for hydraulic actuators. Following examples from biology [12], Raibert's [13] hydraulic legged robots used linear air springs at the leg ends in series with the thrust actuator to recover impact energy when running.

Wells [14] built a hydraulic piston with passive accumulators on each side of the piston chamber which gave the actuator intrinsic compliance. The actuator was better able to tolerate external disturbances.

A Lyapunov-based control algorithm was developed by Alleyne [15] for use in non-linear force control of an Electro-hydraulic actuator. Moderate bandwidth was achieved with an experimental setup as well as in simulation.

Attempts have also been made to infer force output from the pressure in the cylinder. But, pressure fluctuates remarkably in a cylinder and while easy to monitor is very difficult to control. It is also a poor indicator of the actual force on the output due to friction and stiction on the piston and the seals.

Placing a mechanical spring at the end of a hydraulic actuator and measuring the spring's displacement for force control is noticeably absent from the literature.

III. Actuator Model

A. Model

The model we use for the hydro-elastic actuator has a fluid flow input Q from the servo valve and and a position input x_o from the environment on the spring (figure 2). The servo valve is assumed to be first order. Higher order dynamics in the valve are more than an order of magnitude above the frequency range of interest and are therefore neglected. Also, assuming no saturation in the actuator for now, flow is a direct function of input current as seen in equation 1.

$$Q(s) = \frac{K_v}{\tau_v s + 1} i. \tag{1}$$

Saturation effects will be discussed later.

The choice of a position constraint on the spring output has been explained by previous authors in terms of admittance/impedance and position causality of the environment [16], [17], [18].

Even though the physical actuator prototype is not double acting, we will assume that the piston areas are equivalent for ease of analysis and understanding. Having different piston area essentially changes the "transmission ratio" from the fluid to the mechanical domain depending on which side of the piston is pressurized. In the real actuator they are not significantly different from each other and is not important in the analysis shown here. The spring in the model represents a physical die compression spring. It is assumed to be linear in both directions.

The force in the spring, F_l, is a function of two variables: the flow from the servo valve, Q, and the relative

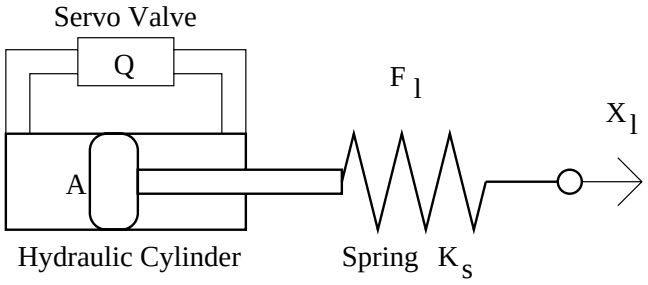

Fig. 2. Simple spring model for the hydro-elastic actuator. The force output of the actuator is determined by the compression of the spring. There are two inputs to the system. Q is the fluid flow from the servo valve. x_l is a position input from the environment.

position of the load, x_l. This relationship is derived to be:

$$F_l(s) = \frac{k_s(Q/A - x_l s)}{s} \tag{2}$$

where k_s is the spring stiffness and A is piston area.

Feedback control of the actuator is closed by measuring the deflection of the spring which implies the force output, F_l, of the actuator. We use a PI controller on the error with controller gain K and integral gain K_i. Even though there is already a free integrator in the open loop system (equation 2), the additional integrator helps to automatically compensate for the wandering null bias offset in the servo valve not accounted for in linear analysis. Assuming that the control gain K has the proper units to take voltage signals F_d (desired force) and F_l (load force) in the spring to current i, control current sent to the servo valve is determined by:

$$i = K(1 + \frac{K_i}{s})(F_d - F_l). \tag{3}$$

This controller puts a pole at the origin and a zero at $-\omega_i$ on the negative real axis where $\omega_i = K_i$.

In our analysis we are interested in the force through the spring which is the force acting on the robot link. Combining equations 1, 2 and 3 yields the closed loop equation for the force through the spring:

$$F_l(s) = \frac{k_s K K_i K_v (s/K_i + 1)F_d - k_s A s^2(\tau_v s + 1)x_l}{As^2(\tau_v s + 1) + k_s K K_v s + k_s K K_i K_v}. \tag{4}$$

With the addition of the integral term in the controller, the closed loop system characteristic equation is now third order.

Equation 4 allows us to look at two cases. For the forward transfer function we assume that the load end is fixed ($x_l = 0$). The other case of interest is at zero force with the load end free ($F_l = 0$). This is the output impedance. The transfer functions for these two cases completely specify the linear characteristics of the actuator.

B. Case 1: Fixed Load

By imposing a fixed end condition on the output and using equation 4, we can write the closed loop forward transfer function for case one which relates the desired force to the output force:

$$\frac{F_l(s)}{F_d(s)} = \frac{k_s K K_i K_v (s/K_i + 1)}{As^2(\tau_v s + 1) + k_s K K_v s + k_s K K_i K_v}. \tag{5}$$

At low frequency, this transfer function is equal to unity, and in the limit as frequency goes to infinity the transfer function goes to zero. We are focusing on driving frequencies significantly less than the servo valve bandwidth. Therefore, the true bandwidth of the system will depend on the servo valve characteristics.

C. Case 2: Free end with zero force

The other case is to assume that the desired force is zero and the output is free to move. This will be the zero load impedance. For case two, we write:

$$\frac{F_l(s)}{x_l(s)} = \frac{-k_s A s^2(\tau_v s + 1)}{As^2(\tau_v s + 1) + k_s K K_v s + k_s K K_i K_v}. \tag{6}$$

Opposite of the closed loop forward transfer function, the impedance at low frequency is equal to zero. This is the property we desire in order to make the actuator very insensitive to position inputs. With active control, the actuator is backdrivable. At high frequency, the transfer function is equal to the value of k_s, the spring constant of the physical spring.

IV. Model Analysis

A. Saturation and Large Force Bandwidth

Regardless of the control system, the open loop characteristics of the actuator will dominate the response when operating at the force and power saturation limits of the servo valve. The maximum flow rate assuming a fully open valve is

$$Q = C\sqrt{P_s - \frac{F_l}{A}} \tag{7}$$

where P_s is the supply pressure, C is a servo valve sizing factor and F_l and A given previously. Equation 7 assumes a negligible return pressure.

Square root saturation is difficult to use in linear analysis. By assuming a linear saturation profile which

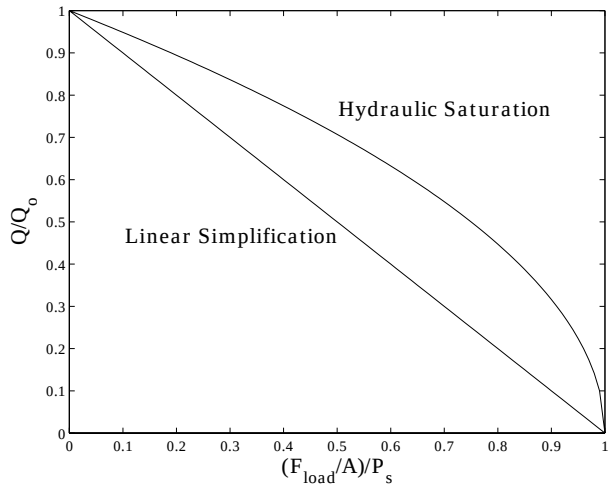

Fig. 3. The actual saturation profile for a hydraulic servo valve is a square root relationship between flow and pressure. In order to understand the effects of saturation on the actuator at a simple level, a linear saturation relationship is assumed.

close to but a worse case than the square root saturation (equation 7), it is possible to understand the effect that the spring has on the large force bandwidth of the actuator (figure 3).

Take the linear saturation profile

$$Q = C_l \left(P_s - \frac{F_l}{A} \right). \tag{8}$$

In this case $C_l = \frac{Q_o}{P_s}$, where Q_o is the maximum flow rate for the rated current of the valve. C in equation 7 and C_l in equation 8 are not equivalent.

As a baseline for understanding the large force or saturation bandwidth, assume that there will be zero load motion and insert the linear flow rate saturation into the open loop dynamic equation for force in the spring (equation 2).

$$F_{l_{max}} = k_s \frac{C_l \left(P_s - \frac{F_{l_{max}}}{A} \right)}{As} \tag{9}$$

Simplifying this equation, we can see that the maximum force possible in the spring follows a first order bandwidth profile.

$$\frac{F_{l_{max}}}{P_s A} = \frac{1}{\frac{A^2}{k_s C_l} s + 1} \tag{10}$$

At low frequency, the system can achieve the maximum force output of the supply pressure times the piston area. However, the capability of the actuator declines sharply after the break frequency

$$\omega_o = \frac{k_s C_l}{A^2}. \tag{11}$$

The careful selection of this frequency is critical to the performance of the actuator. Note that this relationship was made independent of the control system.

B. Dimensionless formulation

In order to generalize and see the effects of the various parameters, both the closed loop transfer function, equation 5, and the output impedance, equation 6, can be written in dimensionless form.

We will normalize frequency about ω_o (equation 11) and generate the following dimensionless groups.

$$\begin{aligned} S &= \frac{s}{\omega_o} \\ I &= \frac{K_i}{\omega_o} \\ V &= \frac{1}{\tau_v \omega_o} \\ \kappa &= \frac{k_s K K_v}{\omega_o A} \end{aligned} \tag{12}$$

- S is a scaled Laplace variable which normalizes s to ω_o.
- I can also be written as ω_i/ω_o. It is the scaled placement of the zero on the negative real axis due to the integral term in the controller.
- V is the scaled time constant from the servo valve first order model. It is a measure of how much faster the servo valve is in comparison to the saturation bandwidth.
- κ represents the scaled loop gain determined by the spring, size of the cylinder, valve gain and controller gain.

Using the dimensionless groups and the scaled Laplace variable, the dimensionless forward closed loop and output impedance transfer functions can be written as:

$$\frac{F_l(S)}{F_d(S)} = \frac{\kappa V (S + I)}{(S + V)S^2 + \kappa V S + \kappa I V} \tag{13}$$

$$\frac{F_l(S)}{k_s x_l(S)} = \frac{-(S + V)S^2}{(S + V)S^2 + \kappa V S + \kappa I V} \tag{14}$$

In order to make the impedance, equation 14, truly dimensionless, it has been normalized to the spring constant k_s.

C. Case 1: Closed Loop

Figure 4 shows a bode plot for equation 13. The plot is normalized to ω_o. For reference, in the real actuator $\omega_o = 152$ rad/sec (25 Hz). The other values used in the plot are $\kappa = 2$, $I = 0.3$ and $V = 4.4$. These values

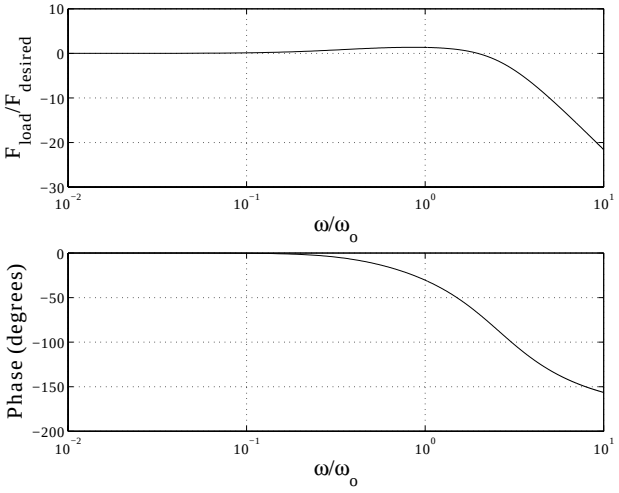

Fig. 4. This is a bode plot of the dimensionless closed loop system scaled to ω_o. Values for the plot were calculated from real parameters on the device: $\omega_o = 152$ rad/sec (25 Hz), $\kappa = 2$, $I = 0.3$ and $V = 4.4$.

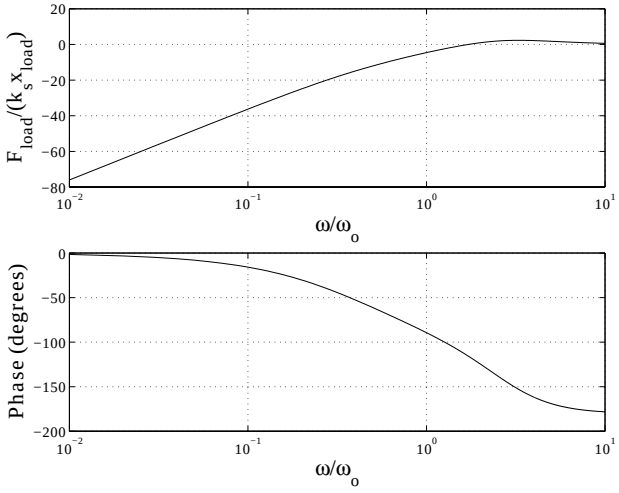

Fig. 5. The impedance of the actuator at low frequency is zero and is k_s at high frequency. The plot represents equation 14. It uses values $\omega_o = 152$ rad/sec (25 Hz), $\kappa = 2$, $I = 0.3$ and $V = 4.4$ which were calculated from the prototype actuator.

are taken from the physical actuator discussed later. At low frequency, the system tracks very well. The system response dies quickly at a frequency above ω_o. The apparent resonance in figure 4 is a strong function of the zero introduced by the control system.

D. Impedance: Case 2

Equation 14 shows the dimensionless form of output impedance. At low frequencies the impedance is zero but in the limit as frequency increases, the impedance is equal to the stiffness of the physical spring, k_s. Equation 14 normalizes to k_s and figure 5 shows an example of the impedance for the same values used in the closed loop forward transfer function in figure 4 and equation 13. In this example, the impedance up to the saturation frequency, ω_o, is significantly reduced.

Ideally the impedance should be as low as possible. There are two ways to accomplish this.

- Increase the control gain.
- Decrease the spring constant.

Increasing the control gain is desirable for increasing the bandwidth of the actuator. Here we see that a larger control gain will also decrease impedance below the cutoff frequency ω_o. At high frequency the impedance will be equal to the stiffness of the spring in the load sensor k_s. The unique part of series elastic actuators is that k_s is relatively low. Increasing the spring constant will actually hurt the impedance. For example, if $k_s \to \infty$ we will have the equivalent of a stiff load cell in series with the output. On the contrary, $k_s \to 0$ will be an actuator with almost zero impedance. Including a compliant spring dramatically reduces the impedance. Nevertheless, there must be a engineering decision which balances the desire for large force bandwidth and low impedance. We discuss this tradeoff further in the next section.

V. Physical Actuator

The following discussion elaborates on decisions made during the design and construction of a prototype hydro-elastic actuator (figure 1). This section also includes experimental results taken from the actuator.

A. Component Selection

The design space for hydro-elastic actuators is very large. Along with geometry and topology there are five major components in addition to the supply pressure source: servo valve, piston, spring, sensor, and controller. Of all five components, choosing the spring is the only part of the actuator which requires unique perspective and is discussed in the next section.

The specifications for the servo valve, piston, and supply pressure need to be done based on the force, speed, and power requirements for a given task. These design requirements are not unique to hydro-elastic actuators and would be done for any hydraulic actuator. It is just important to remember that the bandwidth of the system will be some fraction of the servo-valve bandwidth. Therefore, when choosing the servo valve, it must have sufficient bandwidth to allow for that reduction.

Previous work done on force controllable hydraulics sacrificed seal tolerances on the piston and cylinder to

help reduce stiction and coulomb friction during sliding [13], [14]. In the hydro-elastic actuator, since there is such a large motion to signal ratio, the effects of stiction and friction are virtually eliminated. Therefore, seals can be very tight with little to no degradation in performance.

The other limiting component to achieve high feedback gain is the sensor. The sensor needs to directly measure the spring deflection. This insures that the feedback measurement is a representation of true force regardless of any hysteresis or other losses in the spring. In the prototype, we use a linear potentiometer to measure spring deflection.

B. Choosing the Spring Constant

Selecting the spring constant is a balance between large bandwidth needing a high k_s and impedance needing a low one. We present some guidelines for choosing a spring constant.

1. Select a servo valve, piston, and supply pressure based on the force, speed, and power requirements for the given task. The characteristics of the servo valve will then define the maximum bandwidth of the actuator.
2. Define a minimum acceptable break point ω_o for large force bandwidth. Since the characteristics of servo valve, piston area and spring constant define this value, ω_o defines a lower bound on the stiffness of k_s (section IV-A).
3. Define a minimum tolerable impedance level (section IV-D) which must also come from the task description. This places an upper bound on k_s.
4. Choose a spring within the two set bounds. It may be necessary to iterate. The non-dimensional equations will help in guiding to know whether to increase or decrease k_s and how much effect it will have.

C. Physical Actuator Characteristics

Since this prototype was built as an experimental test bed, it did not have specific task requirements. Nevertheless, as a guideline, we wanted the output power to be 1kW with a max force of 2000N and a max speed of 0.5m/s. Table I shows the actual physical characteristics of the actuator.

We use a MOOG series 30 servo valve with a supply pressure of 20MPa. The 12.5 mm diameter cylinder is from Custom Actuator Products. The springs are Century die compression springs. The actuator output is connected in series with these springs. Regardless of whether the piston is pushing or pulling, the actuator maintains a linear measurable stiffness and deflection. The spring deflection is measured by a Novotechnik linear potentiometer. This measurement is then used in a feedback PI controller which has a desired force input. The output of the controller then defines a control input current to the servo valve.

TABLE I
PHYSICAL PROPERTIES OF PROTOTYPE ACTUATOR

Parameter	A1	A2	Units
Area	1.29	0.97	cm^2
Max. Force	2500	2000	Newton
Cont. Force	2500	2000	Newton
Min. Force	0.5	0.5	Newton
Max Speed	1.25	1.5	m/s
Spring Constant	315	315	kN/m
Max. Power	1500		Watts

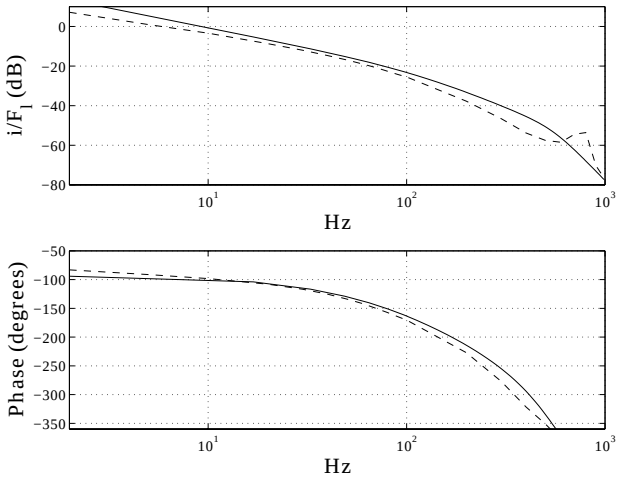

Fig. 6. Open loop response for the servo, piston, spring and sensor. The solid line represents the mathematical model and the dashed line is experimental data. The simulation model uses a full third order servo valve. The model captures all important features except the light damping on 800 Hz resonance.

Frequency response for the open loop system of the servo valve, piston, spring and sensor system is shown in figure 6 for the both mathematical model and experimental setup. The figure is in units of Hertz and is not scaled to the saturation frequency as in the previous section. For the simulation, a full third order servo valve is included in the model. Model and experiment match well in both magnitude and phase. The model even predicts the frequency of the higher order resonance but does a poor job of matching the damping of that pole pair. Nevertheless, since the frequency range of interest is more than an order of magnitude below this frequency, the first order servo valve assumption is justified.

The closed loop actuator experimental frequency response is also very close to the mathematical model.

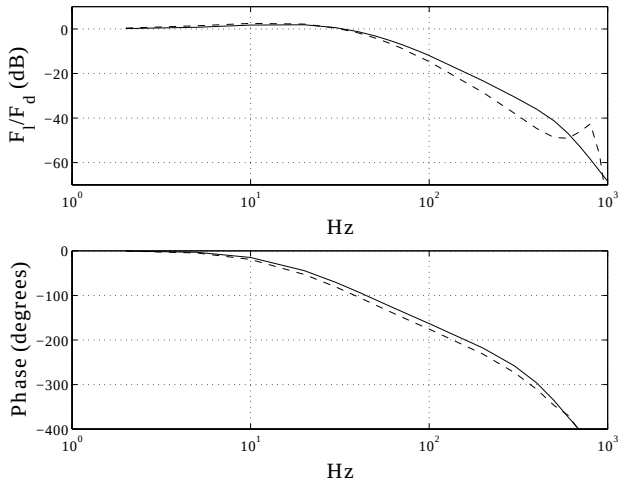

Fig. 7. Closed loop response for the hydro-elastic actuator under PI control. The solid line represents the mathematical model and the dashed line is experimental data. As in figure 6, the simulation model uses a full third order servo valve. The two models match very well in both magnitude and phase for the useful frequency range.

Figure 7 shows the actuator force output response with the fixed end condition (case 1). With the right selection of K and K_i the actuator can achieve a bandwidth that is more than adequate. Again, the 800 Hz pole pair is visible but has no effect on the overall system performance.

Formal impedance measurements have not been performed on the actuator. However, informally one can observe (experience) that it is easy to *backdrive* the actuator with finger force. When the actuator is commanded to output zero force, it responds to the lightest touch. We have also seen that even at higher forces (500 N), the actuator is still *backdrivable*.

In general the prototype actuator performs as expected and verifys that good force control is possible with a hydro-elastic actuator.

VI. Conclusions and Future Work

We use a third order model of a Hydro-Elastic Actuator to investigate the closed loop forward transfer function and the impedance of the system. These two cases completely describe the linear characteristics of the actuator. The model is generalized by using dimensional analysis. We examine force bandwidth and minimizing impedance as a function of controller gain and spring constant.

The model has helped to create a basic design guideline for hydro-elastic actuators with particular emphasis placed on choosing the spring constant for the elastic element. Large bandwidth requires a high spring constant. Minimizing impedance requires a low spring constant. The choice of spring constant has been shown to be a compromise between these competing requirements.

In both the analysis and physical actuator, we use a linear spring. Future work will investigate nonlinear stiffening springs which may ease the design tradeoffs currently required. Further testing will also be done to experimentally verify impedance and saturation.

References

[1] John Hollerbach, Ian Hunter, and John Ballantyne, "A comparative analysis of actuator technologies for robotics," in *Robotics Review 2*. 1991, pp. 299–342, MIT Press.

[2] Gill A. Pratt and Matthew M. Williamson, "Series elastic actuators," *IEEE International Conference on Intelligent Robots and Systems*, vol. 1, pp. 399–406, 1995.

[3] David W. Robinson, Jerry E. Pratt, Daniel J. Paluska, and Gill A. Pratt, "Series elastic actuator development for a biomimetic walking robot.," *IEEE/ASME AIM99*, Sept 20-23, 1999, Atlanta, GA.

[4] H. Hanafusa and H. Asada, "A robotic hand with elastic fingers and its application to assembly process," *IFAC Symposium on Information and Control Problems in manufacturing Technology*, pp. 127–138, 1977, Tokyo.

[5] Matthew Mason, "Compliant motion," in *Robot Motion: Planning and Control*. 1982, pp. 305–322, MIT Press.

[6] Robert H. Cannon Jr. and Eric Schmitz, "Initial experiments on the end-point control of a flexible one-link robot.," *International Journal of Robotics Research*, vol. 3, no. 3, pp. 62–75, 1984.

[7] Mark W. Spong, "Modeling and control of elastic joint robots," *Journal of Dynamic Systems, Measurement, and Control*, vol. 109, pp. 310–319, Dec. 1987.

[8] S. Sugano, S. Tsuto, and I. Kato, "Force control of the robot finger joint equipped with mechanical compliance adjuster," *International Conference on Intelligent Robots and Systems*, pp. 2005–2012, 1992.

[9] H. Asada and K. Youcef-Toumi, *Direct Drive Robots: Theory and Practice*, MIT Press, Cambridge, MA, 1987.

[10] Russel D. Howard, *Joint and Actuator Design for Enhanced Stability in Robotic Force Control*, Ph.D. thesis, Massachusetts Institute of Technology, September 1990.

[11] Matthew M. Williamson, "Series elastic actuators," M.S. thesis, Massachusetts Institute of Technology, June 1995.

[12] R. McNeill Alexander, *Elastic Mechanisms in Animal Movement*, Cambridge University Press, 1988.

[13] Marc. H. Raibert., *Legged Robots That Balance.*, MIT Press, Cambridge, MA., 1986.

[14] D.L. Wells, E.K. Iversen, C.C. Davis, and S.C. Jacobsen, "An investigation of hydraulic actuator performance tradoffs using a generic model," *IEEE International Conference on Robotics and Automation*, pp. 2168–2173, 1990, May 13-18.

[15] Andrew Alleyne, "Nonlinear force control of an electrohydraulic actuator," *Japan/USA Symposium on Flexible Automation*, vol. 1, pp. 193–200, 1996.

[16] Henry M. Paynter, *Analysis and Design of Engineering Systems*, MIT Press, Cambridge, MA, 1960.

[17] N. Hogan, "Impeadance control: An approach to manipulation: Part i - theory, part ii - implementation, part iii - applications," *J. of Dynamic Systems, Measurement and Control*, vol. 107, pp. 1–24, 1985.

[18] C.C. Smith, S.C. Jacobsen, L.A. Robins, D.W. Wilcox, and S.J. Bohn, "Design and control of electromechanical actuation systems," *ASME DSC Modelling and Control of Compliant and Rigid Motion Systems Winter Annual Meeting*, pp. 137–144, 1991, Dec 1-6.